Title

Equivalent Transmission Line Model with a Lumped X-Circuit for a Metalayer Made of Pairs of Planar Conductors

Journal

IEEE Transactions on Antennas and Propagation, 61(2)

ISSN

0018-926X

Authors

Capolino, Filippo
Vallecchi, Andrea
Albani, Matteo

Publication Date

2013-02-01

DOI

10.1109/tap.2012.2225013

Equivalent Transmission Line Model With a Lumped X-Circuit for a Metalayer Made of Pairs of Planar Conductors

Filippo Capolino, *Senior Member, IEEE*, Andrea Vallecchi, and Matteo Albani, *Senior Member, IEEE*

***Abstract*—We present an equivalent X-shaped lumped circuit network to be interposed in the transmission line (TL) modelling reflection and transmission through a recently proposed metalayer in planar technology. The metalayer consists of arrayed pairs of planar conductors that support two main resonant modes, corresponding to either a symmetric or an antisymmetric current distribution in the pairs. The antisymmetric mode is associated with artificial magnetism. We show that reflection and transmission features of a metalayer are accurately predicted by this simple but effective TL model. We also make a clear distinction for the first time between transmission peaks and resonance frequencies, and their relations are investigated in detail. This paper clearly defines the concept of magnetic resonance and identifies the analytical conditions corresponding to total reflection and transmission through a metalayer made of pairs of conductors supporting symmetric and antisymmetric modes.**

***Index Terms*—Artificial materials, arrays, frequency selective surfaces, poles and zeros, transmission lines.**

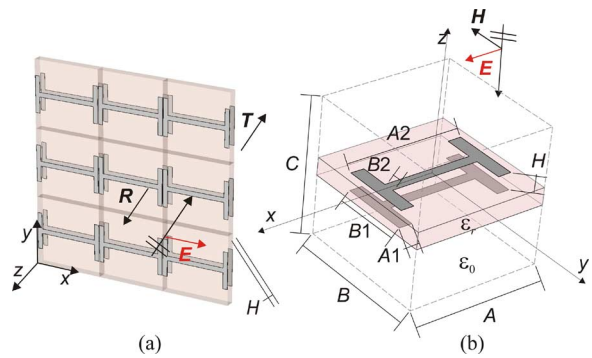

Fig. 1. (a) Perspective view of a metalayer (one layer of the metamaterial) formed by a periodic arrangement of pairs of dogbone-shaped conductors printed on a dielectric substrate. (b) Metamaterial elemental particle (unit cell) with geometrical parameters quoted. The polarization of the incident electric field is along the x-direction.

I. Introduction

PAIRS of finite-length wires have been suggested as constitutive particles for creating a medium with an effective negative refractive index (NRI) [1], [2], alternatively to the conventional combination of split-ring resonators and wires [3], [4]. The pairs of coupled conducting wires exhibit both a "magnetic resonance" (antisymmetric mode) and an "electric resonance" (symmetric mode), that can be partly tuned by adjusting the length of the pair. Later on, the adoption of dogbone-shaped conductors in place of simple cut-wires has been proposed to achieve enhanced control on the particle resonances and to reduce the size of the metamaterial unit cell [4], [5]. As shown in [5], full transmission can be obtained through a single layer (metalayer) of arrayed dogbone-shaped conductor pairs. The observed interesting phenomena seem related to the occurrence of antisymmetric modes in the conductor pairs, which are not present in single layer frequency selective surfaces (FSSs) [13], [14]. Numerical simulations in [6], [7] show that small losses (i.e., $\tan\delta \approx 10^{-3}$) available in commercial dielectric substrates do not significantly affect the total transmission property when the magnetic resonance is not too narrow. The conductor pairing concept has been given a unified point of view in [8], where also pairs of plasmonic nanospheres have been considered. By properly locating the electric and magnetic resonances, it is possible to design composite materials, made of periodic stack of such metalayers, that exhibit artificial magnetism (i.e., effective relative permeability different from unity) or support backward waves [5]–[8].

In this work we describe in detail the features of an equivalent circuit that we have initially proposed in [9], [10] to model the response of a metalayer made of arrayed pairs of conductors (Fig. 1). In this way, a lumped element network is synthesized that when inserted in the plane-wave equivalent transmission line (TL) exhibits the same frequency response of the metamaterial layer. The presence in the metamaterial response of both an electric (symmetric) and a magnetic (antisymmetric) resonance finds its correspondence in two resonant lumped series and parallel *RLC* groups, respectively, arranged in an equivalent balanced X-shaped network [10]. The knowledge of the equivalent network shape and constituents is useful for a description of the layer that can be extended to a wide range of frequencies. Furthermore, we present for the first time an accurate description and precise classification of the transmission and reflection features relative to a metalayer made of arrayed

Manuscript received October 22, 2011; revised August 10, 2012; accepted September 19, 2012. Date of publication October 16, 2012; date of current version January 30, 2013. This work was supported in part by the European Commission FP7/2008, research area "NMP-2008-2.2-2 Nanostructured meta-materials" grant "METACHEM" no. 228762.

F. Capolino is with the Department of Electrical Engineering and Computer Science, University of California Irvine, Irvine, CA 92617 USA (e-mail: f.capolino@uci.edu).

A. Vallecchi was with the Department of Electrical Engineering and Computer Science, University of California Irvine, Irvine, CA 92617. He is now with the Department of Information Engineering, University of Siena, 53100 Siena, Italy.

M. Albani is with the Department of Information Engineering, University of Siena, 53100 Siena, Italy.

Color versions of one or more of the figures in this paper are available online at http://ieeexplore.ieee.org.

Digital Object Identifier 10.1109/TAP.2012.2225013

planar conductor pairs. It is important to note that the magnetic resonance should not be directly associated with a transmission peak. The magnetic resonance is associated with the antisymmetric current distribution which is accurately represented by the *parallel RLC* group in the X-network. This notwithstanding, the transmission peak and the magnetic resonance are closely related phenomena, and in this paper we clarify their relation in detail. Moreover, in the illustrative examples we have analyzed, total reflection does not always occur. We show for the first time that when it occurs, total reflection is at *two* frequencies, one close to the electric resonance and the other close to the magnetic one. Total transmission instead, if it occurs, is located near the magnetic resonance. This latter case is particularly important because it is related to the matching properties of the metalayer to a wave in free space. For the first time we determine the analytical conditions corresponding to the occurrence of total reflection and total transmission. We also introduce the quality factors of the electric and magnetic resonances, and we use them to explain the two phenomena of total reflection and transmission.

The knowledge of an equivalent network (shape and constituents) is necessary to parameterize with the least number of physical parameters the frequency behavior of a metalayer made of arrayed pairs. It opens up possibilities to improve metalayers performance in terms of matching, bandwidth, and interaction with other dielectric layers, similarly to the advantage one obtains when representing a FSS in terms of circuits, as clearly shown in [12], [13]. The proposed X-network can be regarded as a low-order expansion in terms of frequency poles and zeros of the impedances representing the two-port metalayer. The representation that we have chosen is made in terms of physically realizable parameters since each network elements satisfies the Foster theorem [14], [15]. In general, a TL approach is a powerful tool. For example it has been able to correctly model enhanced transmission through an array of subwavelength slits in a film, at optical [16] and microwave [17] frequencies.

II. The Equivalent Z-Transmission Line Model for a Layer of Pairs

The planar metalayer analyzed in this paper, composed of a periodical arrangement of pairs of dogbone-shaped conductors, is depicted in Fig. 1.

As an illustrative and introductory example, we consider the reflection and transmission of a normally incident wave through a single layer of dogbone pairs (Fig. 1) with a dielectric spacer of relative permittivity $\varepsilon_r = 3.48$ and $\tan\delta = 0.004$ (e.g., Rogers RO4350) and the following unit cell and conductor dimensions in mm (cf. Fig. 1(b)): $A = 7.5, B = 7.5, A1 = 0.8, B1 = 4, A2 = 7.4, B2 = 0.8, H = 0.8$. The transmission and reflection coefficients, T and R, as obtained by numerical full wave (FW) simulations (CST Microwave Studio), are plotted in Fig. 2(a).

In accordance with the dogbone-pair particle phenomenology discussed in detail in [4], [5], each pair supports two fundamental resonances: the symmetric resonance (also denoted as *electric resonance*) that determines the stopband around $f_e \approx 6.89$ GHz, and the antisymmetric resonance (also denoted as *magnetic resonance*) that is mainly responsible for the transmission peak around $f_m \approx 6.33$ GHz. Fig. 2(b) shows the currents at 6.33 GHz, induced by an illuminating plane wave, that is dominated by the antisymmetric mode and thus produces an equivalent magnetic dipole along the y-direction.

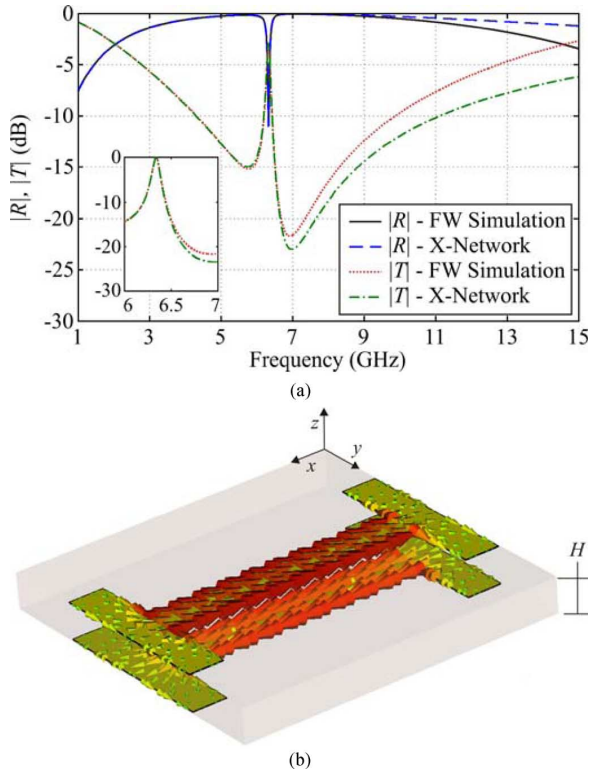

Fig. 2. (a) Transmission coefficient vs. frequency for a metalayer, i.e., a layer of dogbone pairs separated by a dielectric spacer with $\varepsilon_r = 3.48$ and $\tan\delta = 0.004$: the *magnetic* resonance is around $f_m \approx 6.33$ GHz, whereas the *electric* resonance is at $f_e \approx 6.89$ GHz. Total transmission (in the lossless case shown in the inset zoom) occurs near f_m. Total reflection never occurs. Data from a full wave (FW) numerical analysis (CST) are compared with those from the proposed equivalent X-network. (b) Antisymmetric current in a pair, excited by a plane wave at $f = 6.33$ GHz.

From Fig. 2 one can notice that because of the presence of a small amount of metal and dielectric losses, total transmission (zero reflection) does not occur near f_m. We have also noticed that larger values of H would result in $|T|$ closer to unity [6], [7]. Instead, in the absence of losses, one would have exactly $|T| = 1$ near f_m, as apparent from the inset of Fig. 2(a) showing T for the above dogbone metalayer in the case of a lossless dielectric spacer and perfect electric conductors. A detailed explanation for this will be provided in Section III. One should note the close similarity of the isolated transmission peak near $f \approx 6.3$ GHz to the Fano resonance [19] discussed in other studies, as for example in [20], [21], and to the electromagnetic induced transparency (EIT) phenomenon [22]. In metamaterial-based problems, both the Fano resonance and the EIT have been related to "dark modes" [22], [23], which weakly couple to external fields, or weakly scatter, as it happens for the antisymmetric mode here analyzed. In general, the weak coupling of a dark mode to external fields is due to small asymmetries. In our case the asymmetry is represented by the small phase shift that

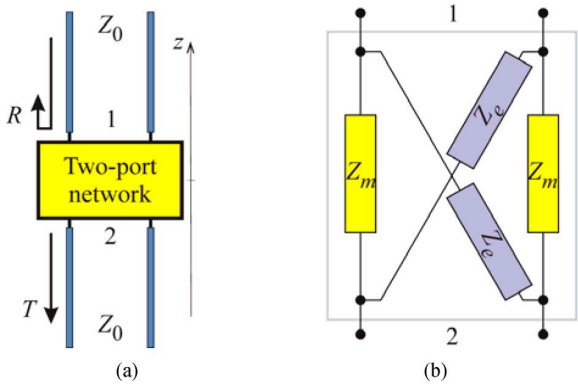

Fig. 3. (a) Plane-wave equivalent z-transmission line with the two-port network representing the metamaterial layer. (b) Synthesized two-port symmetric X-network, reproducing the metalayer frequency response, which comprises two *RLC* groups associated to the metamaterial electric and magnetic resonances.

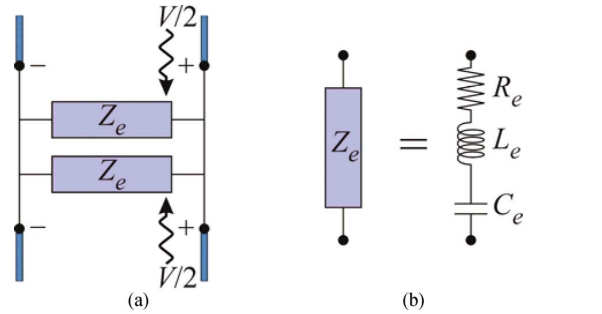

Fig. 4. (a) TL model equivalent network for a periodic surface of dogbone pairs under symmetric (even) excitation. (b) Series resonant *RLC* circuit representation for the electric mode impedance.

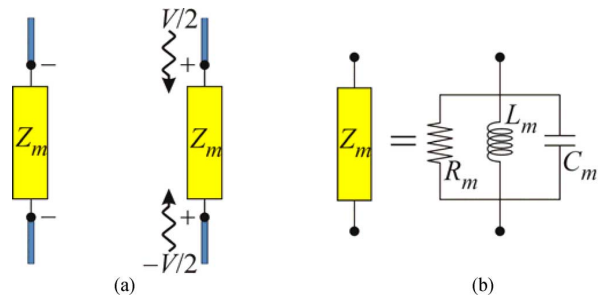

Fig. 5. (a) TL model equivalent 2-port network for a periodic surface of dogbone pairs under antisymmetric (odd) excitation. (b) Parallel resonant *RLC* circuit representation for the magnetic mode impedance.

an incident plane wave has between the top and bottom conductors of the pair. It is well known indeed, that an antisymmetric mode with small height H results in weak coupling to external fields or in weak scattering. The very small scattering implies that the antisymmetric mode (magnetic resonance) is a narrow band phenomenon, contrarily to the symmetric mode that scatters as an electric dipole and constitutes a wider band phenomenon. As discussed in Section III, the resonance of the antisymmetric mode therefore has a large quality factor, whereas the resonance associated with the symmetric mode has a significant lower one because of the higher radiation "losses".

The purpose of what follows is to provide a z-TL model capable of describing the fundamental electric and magnetic resonances induced by a normally incident plane wave in a metalayer of paired conductors, as the one shown in Fig. 1. The TL model will accurately reproduce the low-frequency portion of the metalayer reflectance and transmittance spectra in Fig. 2(a). In particular, the equivalent TL model consists of the equivalent 2-port network shown in Fig. 3 made by lumped elements. It is well known that such a network model can effectively describe the response of the structure in the low frequency range; i.e., until the unit cell period is small compared to the wavelength. The equivalent circuit can be retrieved by fitting the reflection/transmission response of the structure. However, the choice of an unsuitable circuit topology would result in a nonphysical behavior for some of the impedance/admittance of the lumped elements (e.g., a non Foster frequency dependence). A good strategy to arrange a proper circuit topology, resulting in physically behaving lumped elements, is to have the circuit elements directly represent the physical behavior (in terms of local magnetic and electric fields) of the various parts of the unit cell geometry. For example, as well known [12], [13], [15], an effective model for the *single layer* of dogbones is just a lumped *LC*-series shunt element, where the inductance is associated with the current on the central strip of the dogbone, and the capacitance with the gap between the ends of two consecutive dogbones. These concepts have been used extensively in designing FSSs, and circuit parameters have been also used to design dielectric layers to modify the FSS frequency response [12].

We have found that the topology in Fig. 3(b) is a possible two-port network representation modeling a metalayer of paired conductors. In order to better understand the adopted network topology, it is useful to analyze its behavior under *symmetric* (even, Fig. 4) and *antisymmetric* (odd, Fig. 5) excitations. In such cases the structure response is simpler because it is dictated only by either the symmetric or the antisymmetric mode, respectively. Then, by using the superposition principle, one can combine the two results corresponding to the above elemental symmetries to describe the case of general excitation, still preserving circuit compactness and simplicity of analysis.

When the dogbone pair is excited *symmetrically* by two in-phase plane waves that impinge from opposite directions and have the same phase at $z = 0$ (i.e., in the middle of the pair), the perfect symmetries of the structure and excitation result in a symmetric response (symmetric mode) with respect to the $z = 0$ plane. Indeed, the transverse (x, y) electric field components and the z component of the magnetic field exhibit an even z dependence; conversely the electric field z component and the transverse magnetic field components are odd functions of z. Therefore the symmetry plane at $z = 0$ is virtually a perfect magnetic conducting plane. As a consequence, voltages and currents across corresponding shunt elements Z_e in the two upper and lower branches of the equivalent network in Fig. 3(b) are the same, whereas voltage drop and current through series elements Z_m vanish so that they can be deleted. Therefore the equivalent network in Fig. 3(b) reduces to the simpler configuration in Fig. 4(a). Under this *symmetrical* excitation the behavior of the dogbone pair is similar to that

of a single dogbone which is effectively modeled by a series resonant *RLC* circuit, as shown in Fig. 4(b).

An analogous simplified analysis can be performed for the *antisymmetric* excitation case, where the two plane waves impinging from opposite directions are in counterphase at $z = 0$. Now, all the symmetries are exchanged; i.e., the transverse (x, y) electric field and the z-polarized magnetic field components are odd functions of z, while the z-polarized electric field and transverse (x, y) magnetic field components exhibit an even z dependence. Accordingly, the symmetry plane is now a virtual perfect electric conducting plane, and the antisymmetric response of the dogbone pair is equivalent to the response of a grounded (single) dogbone structure. Again, the equivalent network in Fig. 3(b) can be reduced. Because of symmetry, the resulting total series impedance $2Z_m$ on the right arm is halved and each arm of the network is assigned an impedance Z_m, without affecting the balanced response, thus obtaining the simplified circuit in Fig. 5(a). It is found that an appropriate response for Z_m can be represented by the simple parallel resonant *RLC* circuit shown in Fig. 5(b) that fits the low frequency behavior of the metalayer and its first magnetic resonance.

According to the above analysis, the electric and magnetic impedances in the X-network are the series and parallel resonant *RLC* circuits in Figs. 4(b) and 5(b), respectively, described by

$$\frac{1}{Z_m} = \frac{1}{R_m} + \frac{1-\omega^2/\omega_m^2}{j\omega L_m}, \quad Z_e = R_e + \frac{1-\omega^2/\omega_e^2}{j\omega C_e} \tag{1}$$

where ω is the angular frequency and

$$\omega_m = 2\pi f_m = \frac{1}{\sqrt{C_m L_m}}, \quad \omega_e = 2\pi f_e = \frac{1}{\sqrt{C_e L_e}}, \tag{2}$$

denote the *magnetic* and *electric* resonance, respectively. Indeed, the proposed X-network is consistent with the usual model of the stop band response of capacitive FSSs, that can be represented as a *LC* series resonant circuit [12], [15], and previous knowledge about the magnetic resonance that in [5] was described by a *LC* resonator. The presence of losses in the metals and/or the dielectric spacer is taken into account by the resistive lumped elements in the *LC* series and parallel resonant circuits Z_e and Z_m, which become *RLC* circuits.

The calibration of the circuital elements involved in the adopted equivalent network topology is accomplished by referring to its Z-parameter representation [12], where the impedance terms Z_{ij} are simply related to Z_m and Z_e of the X-shaped network as

$$\underline{\mathbf{Z}} = \begin{bmatrix} Z_{11} & Z_{12} \\ Z_{21} & Z_{22} \end{bmatrix} = \frac{1}{2}\begin{bmatrix} Z_e + Z_m & Z_e - Z_m \\ Z_e - Z_m & Z_e + Z_m \end{bmatrix}. \tag{3}$$

The Z-parameters are evaluated from the S-parameters [25] determined by FW simulations, whence $Z_m = Z_{11} - Z_{12}$ and $Z_e = Z_{11} + Z_{12}$.

As an example, in Fig. 6 we show the impedances Z_m and Z_e of the X-network synthesized for the layer of dogbone pairs relative to the case in Fig. 2(a). The real and imaginary parts of the reference Z_m and Z_e impedances derived from the FW simulations are plotted in solid black and dotted red lines, respectively, in Fig. 6. The R, L, and C parameters in the representations (1) of Z_m and Z_e of the X-network (Fig. 3) are obtained

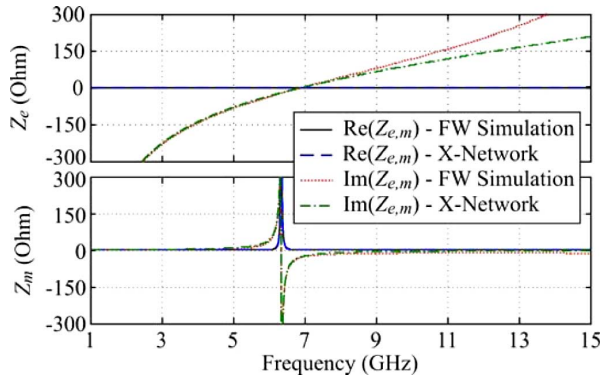

Fig. 6. Impedances Z_m and Z_e evaluated from the impedance parameters Z_{ij} computed by FW simulations superimposed with the impedances Z_m and Z_e synthesized via the *RLC* circuits and calibrated by fitting the FW data.

by fitting the magnetic resonance frequency and bandwidth, for Z_m, and the electric resonance frequency and the impedance value at a lower frequency, for Z_e, of the corresponding FW results. Specifically, for the dogbone pair array in the case in Fig. 2(a) we have[1]

$$\begin{aligned} C_m &= 5.4696\ \text{pF}, \quad L_m = 0.1154\ \text{nH}, \quad R_m = 944.74\ \Omega \\ C_e &= 0.1895\ \text{pF}, \quad L_e = 2.8158\ \text{nH}, \quad R_e = 0.573\ \Omega. \end{aligned} \tag{4}$$

The good agreement in Fig. 6 between the synthesized impedances Z_m, Z_e and those retrieved from FW simulations in the low frequency range confirms the validity of the representations (1) and the effectiveness of the network topology we have adopted. However, since higher order resonances are not taken into account in this equivalent network, increasingly larger discrepancies between the X-network impedances and the corresponding quantities derived from FW results inevitably appear for increasing frequencies. It is noted that $C_m \gg C_e$ and $L_m \ll L_e$; therefore, the resonance frequency f_m can be of the same order of f_e.

Once retrieved the impedances Z_m and Z_e, the scattering parameters of the X-network (reflection R and transmission T, for this symmetric structure) can be calculated through the formulas

$$R = \frac{Z_e Z_m - Z_0^2}{\Delta}, \quad T = \frac{(Z_e - Z_m)Z_0}{\Delta} \tag{5}$$

$$\Delta = (Z_m + Z_0)(Z_e + Z_0). \tag{6}$$

The results in Fig. 2(a) show that the transmission and reflection coefficients predicted by using the z-TL model with the X-shaped network correctly reproduce the original FW simulation results. The electric and magnetic frequencies are now determined as $f_m = 6.335$ GHz, and $f_e = 6.89$ GHz. Observation of the results in Fig. 2(a) confirms that the electric frequency f_e corresponds to the location of the deep and wide stop band. Moreover, the magnetic frequency f_m approximately corresponds to the location of the maximum of transmission, or

[1]Circuit parameters are specified with 4 significant digits for the sole purpose of consistently computing resonance frequencies. Only in some cases that precision is required to quantify the very small distances from the relative matching/mismatching frequencies (that can be very close to the electric and magnetic resonances).

more properly to the frequency range where large and rapid variations of the reflection and transmission coefficients occur.

It is important to note that the correct values of Z_m and Z_e, and in turn of R and T, can be reconstructed using physically realizable values of $R_{e,m}$, $L_{e,m}$ and $C_{e,m}$. Also, employing classical Π or T two-port network topologies would have entailed the need of using non-physically realizable network elements (i.e., not satisfying the Foster's theorem). For example, in the T topology the shunt element corresponds to the impedance Z_{21} which, at the magnetic resonance, exhibits a negative slope of the imaginary part, in contradiction with Foster's theorem for reactive impedances.

Finally, it is noteworthy that the extension of the proposed equivalent network model to the case of oblique propagation can be accomplished by describing the angular dependence of the impedances Z_m and Z_e through the approach described in [18].

III. Resonances and Matching Conditions

We are interested in analyzing the resonances and the free space matching and mismatching conditions for one layer of arrayed dogbone pairs illuminated at normal incidence by a plane wave with the electric field polarized along the direction of the dogbone central conductor, as shown in Fig. 1(b). We will clearly show how plane wave reflection and transmission properties are related to the electric and magnetic resonances, and by using the X-network we will determine the conditions for absence of transmitted or reflected waves. Most of the results and concepts described here for an array of dogbone pairs are still valid for other paired geometries, as long as they support symmetric and antisymmetric modes. In this section, to illustrate the main trends also with the help of closed form formulas, we will assume absence of losses (i.e., $R_e = 0$ and $R_m \to \infty$), since these can be neglected in various cases at microwave frequencies, especially if the spacer thickness H is not too small [6], [7].

Near the magnetic resonance one may observe two opposite behaviours: $|R| = 1$ and $|T| = 1$, treated in the following Subsections C and D, corresponding to the narrowband peaks near the magnetic resonance in the transmission plots shown in Section IV. It is important to observe that in the example considered in the previous section, as well as in those of the next section, which are representative of a large variety of configurations, it always results $L_m \ll L_e$ and $C_m \gg C_e$, but the electric and magnetic resonance frequencies are of the same order. Accordingly, the series impedance Z_m in the X-network is the parallel of two low impedances, $j\omega L_m$ and $1/(j\omega C_m)$, and its magnitude is generally small with respect to the free space impedance Z_0 (Fig. 6), except very near and at the magnetic resonance ($f \approx f_m$), where Z_m is singular (assuming a lossless case). Conversely, the cross impedance Z_e is the series of two large impedances, $j\omega L_e$ and $1/(j\omega C_e)$, which are comparable or larger than Z_0. Therefore, the magnitude of Z_e is comparable or larger thanZ_0, except near and at the electric resonance ($f \approx f_e$) where it vanishes, as shown in Fig. 6.

A. Electric Resonance f_e ($Z_e = 0$)

At the frequency f_e, for which the LC series electric impedance resonates, $Z_e = 0$; consequently the equivalent circuit simplifies as in Fig. 7(a), and the reflection and transmission coefficients (5) for one layer of arrayed conductor pairs reduce to

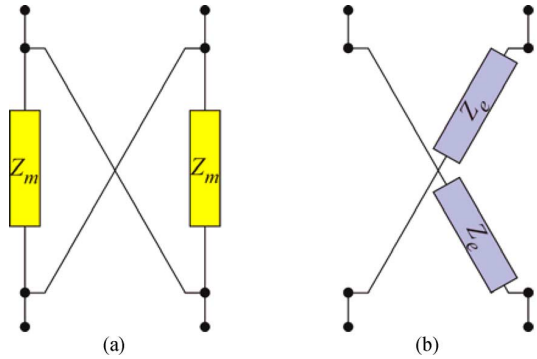

Fig. 7. Reduction of the X-network at (a) the electric resonance when $Z_e = 0$, and (b) the magnetic resonance when $Z_m = \infty$.

$$R = \frac{-Z_0}{Z_m + Z_0}, \quad T = \frac{-Z_m}{Z_m + Z_0}, \tag{7}$$

Since usually $|Z_m| \ll Z_0$ (except near the magnetic resonance frequency f_m of the parallel of L_m and C_m), the TL is almost short circuited at the port section, and therefore $T \approx 0$, and $R \approx -1$. However, when Z_m is not that small (e.g., $|Z_m| \approx Z_0$) the transmission coefficient does not vanish, as for example in Fig. 2(a) at $f = f_e$. On the other hand, if the electric resonance falls very close to the magnetic one, besides $Z_e = 0$ we also have that $|Z_m| \gg Z_0$ at $f \approx f_m$, and rather than short circuited the TL is matched to the TL after port 2. In this case, we have nearly full transmission $T \approx -1$ (the negative sign is because of the inverter in Fig. 7(a)), and $R \approx 0$. This condition is hardly met because the magnetic resonance is very narrow.

In summary, at the electric resonance frequency f_e (i.e., when $Z_e = 0$), if the magnetic resonance is far from the electric one, we have almost total reflection; instead, when the magnetic resonance is very close to the electric one (i.e., $f_m \approx f_e$), we have a narrow passband at $f = f_e \approx f_m$.

B. Magnetic Resonance f_m ($Z_m = \infty$)

At the frequency f_m the LC parallel magnetic impedance resonates and $Z_m = \infty$; consequently, the equivalent circuit simplifies as in Fig. 7(b), and the reflection and transmission coefficients (5) for one layer of arrayed pairs reduce to

$$R = \frac{Z_e}{Z_e + Z_0} \quad \text{and} \quad T = \frac{-Z_0}{Z_e + Z_0}. \tag{8}$$

Since generally Z_e is of the same order of Z_0 (or at least Z_e is significantly different from zero except near the electric resonance), the TL is terminated on a poorly matched load at the port section, and therefore exactly at $f = f_m$ the transmission is small while the reflection is considerable. However, when the electric resonance is close to the magnetic one (i.e., $f_e \approx f_m$), one has $|Z_e| \ll Z_0$ at $f = f_m \approx f_e$, which corresponds to the interesting effect of full transmission with $T \approx -1$ and $R \approx 0$ that we have previously described.

Anyway, *near* (but not at) the magnetic resonance opposite phenomena occur because of the large variation of Z_m, as explored in detail in the next two subsections.

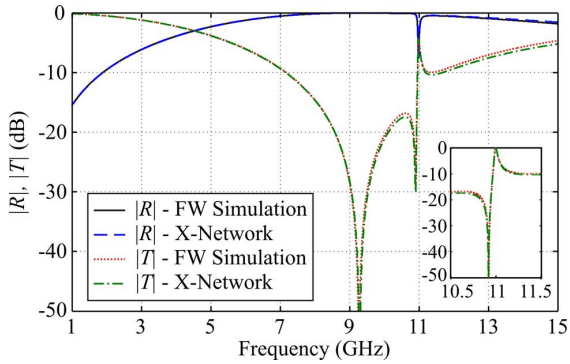

Fig. 8. Transmission coefficient vs. frequency for a layer of dogbones pairs separated by a spacer with $\varepsilon_r = 1$. (ε_r is the relative permittivity of the dielectric between the pair of conductors.) The *magnetic* resonance is at $f_m \approx 11$ GHz, whereas the *electric* resonance is at $f_e \approx 9.2$ GHz. Total transmission (in the lossless case shown in the inset zoom) occurs near f_m. Two total reflections occur: one near f_m, the other near f_e. Data from FW simulations (CST) are compared with those from the proposed equivalent X-network.

C. Matching Resonance f_T: Total Transmission ($R = 0, |T| = 1$)

Using the TL analogy shown in Figs. 6–8, the condition for absence of reflection ($R = 0$) is seen from (5) to be fulfilled both at $f \to 0$ and $f \to \infty$. Indeed for both $f \to 0$ and $f \to \infty$, $Z_m \to 0$ and $Z_e \to \infty$, so that $R = 0$. However, the low frequency regime is usually below the operating frequency range and the high frequency regime is beyond the validity of the model. Here, we are interested in determining necessary and sufficient conditions for absence of reflection at a frequency near the magnetic resonance. Imposing $R = 0$ in (5), absence of reflection occurs at the radiant frequency ω_T for which

$$Z_m Z_e = Z_0^2. \tag{9}$$

Inserting this condition in (5) gives

$$T = \frac{\sqrt{Z_e} - \sqrt{Z_m}}{\sqrt{Z_e} + \sqrt{Z_m}} = \frac{Z_e - Z_0}{Z_e + Z_0} = \frac{Z_0 - Z_m}{Z_0 + Z_m}. \tag{10}$$

In a lossless structure Z_m and Z_e are purely imaginary, and therefore (10) confirms that absence of reflection corresponds to total transmission $|T| = 1$. A matching resonance f_T is generally found near the magnetic resonance, where condition (9) is likely met because of the large range of values assumed by Z_m. Indeed, to satisfy (9) Z_m and Z_e must be of opposite sign (one capacitive and the other inductive), as it occurs in the low and high frequency regions below and above the electric and magnetic resonances. Hence, f_T cannot fall between the two resonances where Z_m and Z_e have the same sign (both capacitive or both inductive). More specifically, the matching condition (9) is elaborated as

$$a\left(\frac{1 - f^2/f_e^2}{1 - f^2/f_m^2}\right) = 1 \tag{11}$$

where

$$a = \frac{L_m}{C_e}\frac{1}{Z_0^2} = \frac{Q_e}{Q_m}\frac{f_e}{f_m} \tag{12}$$

and we have introduced the quality factors of the parallel magnetic resonance $Q_m = Z_0\sqrt{C_m/L_m}$ and of the series electric resonance $Q_e = \sqrt{L_e/C_e}/Z_0$. Examining the sign of the expression on the left hand side, we deduce that the matching condition may be encountered at either $f_T < f_e, f_m$ or $f_T > f_e, f_m$, as already observed above. It is useful to define also

$$b = \frac{L_e}{C_m}\frac{1}{Z_0^2} = \frac{Q_e}{Q_m}\frac{f_m}{f_e} = a\frac{f_m^2}{f_e^2}. \tag{13}$$

To determine the necessary and sufficient conditions for the existence of the matching frequency f_T, we rearrange (11) as

$$f^2 = f_m^2\frac{1-a}{1-b} = f_e^2\frac{1-1/a}{1-1/b}. \tag{14}$$

It is clear that a real f solution of (14) and (11) always exists for the two cases $a, b > 1$ and $a, b < 1$.

In particular, when $f_m > f_e$ (i.e., $b > a$) two important subcases must be distinguished. When $a < b < 1$, then $(1-a)/(1-b) > 1$ and a solution exists for $f_e < f_m < f_T$, whereas when $1 < a < b$, then $(1-1/a)/(1-1/b) < 1$ and a solution exists for $f_T < f_e < f_m$, There are no real f solutions of the matching condition when $b > 1 > a$.

Analogously, when $f_m < f_e$ (i.e., $b < a$) we must distinguish between two subcases. When $b < a < 1$, then $(1-a)/(1-b) < 1$ and a solution exists for $f_T < f_m < f_e$, whereas when $1 < b < a$, then $(1-1/a)/(1-1/b) > 1$ and a solution exists for $f_m < f_e < f_T$, There are no real f solutions of the matching condition when $b < 1 < a$.

From (14), the matching resonance f_T satisfying (11) can be expressed as

$$f_T = f_m\sqrt{\frac{1-a}{1-b}} = f_e\sqrt{\frac{1-1/a}{1-1/b}}. \tag{15}$$

The various conditions for matching are summarized in Table I. Since in most cases the magnetic resonance is narrowband, and thus $Q_m/Q_e \gg 1$, it follows that $a, b \ll 1$ and (15) can be approximated as

$$f_T \approx f_m + f_m\frac{(b-a)}{2} \tag{16}$$

which shows that the matching condition generally occurs *close* to the magnetic resonance.

1) Wideband Transparency. Case $f_e = f_m$ ($a = b$): Since both cases $f_m < f_e$ and $f_m > f_e$ are admissible, we can argue that also the case $f_e = f_m$ is possible, which would implies $a = b$. At this coincidence of the electric and magnetic resonances, if it is also verified that $a = b = 1$, i.e., $Q_m = Q_e$, then $R = 0$ for any frequency and indeed the layer would exhibit a wideband transparency. However, in practical designs like those explored in this paper, $Q_m \gg Q_e$ and the condition $Q_m = Q_e$ is far to be reached.

TABLE I
TOTAL TRANSMISSION PEAK (MATCHING CONDITION) LOCATION

Electric/magnetic resonance order	$a, b < 1$	$a, b > 1$	$a < 1 < b$ $b < 1 < a$
$f_e < f_m$ $(a < b)$	$f_m < f_T$	$f_T < f_e$	No solution
$f_m < f_e$ $(b < a)$	$f_T < f_m$	$f_e < f_T$	No solution

D. Mismatching Resonance f_R: Total Reflection ($T = 0, |R| = 1$)

The total mismatching condition is here defined as absence of transmission $T = 0$. According to (5), the mismatch happens when $Z_e = Z_m$, which, implies that

$$R = \frac{Z_e - Z_0}{Z_e + Z_0} = \frac{Z_m - Z_0}{Z_m + Z_0}. \tag{17}$$

In a dual manner with respect to the preceding case of the matching resonance, since in a lossless structure both Z_m and Z_e are purely imaginary, (17) confirms that absence of transmission corresponds to total reflection $|R| = 1$. Moreover, as stated above, the quality factor Q_m of the magnetic resonance is generally much higher than that of the electric resonance Q_e. This implies that $Z_m \ll Z_e$, except that very close to the magnetic or electric resonance; therefore, the condition $Z_m = Z_e$ may occur at two frequencies f_R that are (*i*) near the electric resonance, or (*ii*) near the magnetic resonance, as explained next. (*i*) Near the electric resonance, Z_e assumes small positive or negative imaginary values, which is characteristic of a resonant series LC circuit. Therefore, either immediately below or above the electric resonance frequency, the condition of total reflection $Z_e = Z_m$ may occur (elsewhere one has $Z_m \ll Z_e$). In this case f_R is near the electric resonance f_e (defined as $Z_e = 0$), and at $f = f_R \approx f_e$ one has $Z_e \approx 0$ and thus $R \approx -1$. In this case the mismatch resonance corresponds to the wideband large standard-FSS-like reflection associated with the electric resonance observed in all the transmission plots.

(*ii*) Near the magnetic resonance, Z_m undergoes the large impedance variation typical of a resonant parallel LC circuit. Therefore, either immediately below or above the magnetic resonance frequency, the condition of total reflection $Z_e = Z_m$ may occur (elsewhere one has $Z_m \ll Z_e$). In this case f_R is close to the magnetic resonance f_m (defined as $Z_m = \infty$), and at $f = f_R \approx f_m$ one has that $Z_m \approx \infty \gg Z_0$ and thus $R \approx 1$. In this case, the metalayer made of paired conductors tends to approximate an artificial magnetic wall. This phenomenon is not encountered in standard FSSs and is related to the excitation of strong antisymmetric currents in paired patterned structures. In general, this phenomenon is narrowband because the variation with frequency of Z_m is very rapid.

In summary, one may have two mismatch frequencies f_R: when $f_R \approx f_e$ one has $T = 0$ and $R \approx -1$, whereas when $f_R \approx f_m$ one has $T = 0$ and $R \approx 1$. The last condition is a new phenomenon due to the presence of strong antisymmetric currents in bilayered patterned FSSs, as already observed and explained in [5]–[7].

A further important property that needs to be assessed is the location of the two total reflection frequencies f_{R1} and f_{R2} with respect to the electric and magnetic resonances. A distinction is made based on the order of the electric and magnetic resonances, i.e., depending whether $f_e < f_m$ or $f_m < f_e$. The sign of the imaginary part of the impedances is as follow: for the electric resonance $\mathrm{Im}(Z_e) < 0$ for $f < f_e$ and $\mathrm{Im}(Z_e) > 0$ for $f > f_e$. For the magnetic resonance $\mathrm{Im}(Z_m) > 0$ for $f < f_m$ and $\mathrm{Im}(Z_m) > 0$ for $f > f_m$. Therefore, considering that $Q_m \gg Q_e$, if $f_e < f_m$ the total reflection condition $Z_e = Z_m$ can be satisfied at f_{R1} and f_{R2} in the frequency region $f_e < f_{R1,2} < f_m$. Vice versa, if $f_m < f_e$, the total reflection condition $Z_e = Z_m$ can be satisfied at f_{R1} and f_{R2} in the frequency region $f_m < f_{R1,2} < f_e$.

TABLE II
LOCATION OF THE TWO TOTAL REFLECTION PEAKS f_{R1}, f_{R2}. ONE IS ALWAYS NEAR THE MAGNETIC RESONANCE f_m

Electric/magnetic resonance order	Total reflection peaks location
$f_e < f_m$	$f_e < f_{R1,2} < f_m$
$f_m < f_e$	$f_m < f_{R1,2} < f_e$

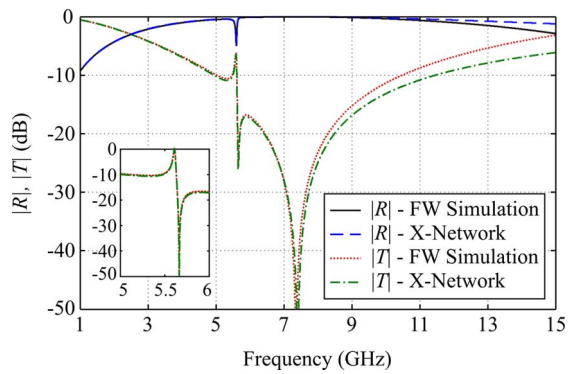

Fig. 9. Reflection and transmission coefficients vs. frequency for a layer of dogbones pairs separated by a spacer with $\varepsilon_r = 4.5$ and $\tan\delta = 0.002$. The *magnetic* resonance is at $f_m = 5.603$ GHz, whereas the *electric* resonance is at $f_e = 7.47$ GHz. Total transmission (in the lossless case shown in the inset zoom) occurs near f_m. Two total reflections occur: one near f_m, the other near f_e. Data from FW simulations (CST) are compared with those from the proposed equivalent X-network.

This trend is summarized in Table II and can be clearly observed in Fig. 8 and in Fig. 9, as well as in Fig. 12 of [5]. In certain cases, as for example in Fig. 2, and in [5], a total reflection is not observed; this aspect is clarified in the following.

In the transmission plots in Figs. 8 and 9 the rapid variation at 11 and 5.6 GHz, respectively, (sometimes referred to as an antiresonance) is associated with the magnetic resonance. Though in the past literature this antiresonance has been loosely associated with a magnetic resonance, the above discussion more precisely offers the possibility to estimate whether the actual magnetic resonance f_m is located at a frequency smaller or larger than that corresponding to the peak of total reflection (absence of transmission).

Finally, it is interesting to show under which conditions total reflection occurs (e.g., it does not occur in Fig. 2, whereas it does occur in Figs. 8 and 9). This is done by solving for f the equation $Z_e = Z_m$, using the expressions given in (1), which leads to

$$\left(1 - \frac{f^2}{f_m^2}\right)\left(1 - \frac{f^2}{f_e^2}\right) = -4\pi^2 L_m C_e f^2. \tag{18}$$

This equation has been derived by neglecting losses, and it admits either two real solutions or none. Following the steps in the

Appendix, two real solutions of $Z_e = Z_m$ can be found if and only if

$$Q_m Q_e \geq \frac{f_e f_m}{(f_e - f_m)^2} \tag{19}$$

and the mismatching frequencies are given by

$$f_{R1,2} = \frac{1}{\sqrt{2}} \sqrt{B \pm \sqrt{B^2 - 4 f_e^2 f_m^2}} \tag{20}$$

where $B = f_e^2 + f_m^2 - f_e f_m / (Q_m Q_e)$. When $Q_m Q_e \gg 1$, it is easy to verify from (20) that the two solutions are $f_R \approx f_e$ and $f_R \approx f_m$ as previously noticed.

IV. Discussion and Examples of Metalayers of Dogbone Pairs

The example in Fig. 2(a) (*Case 1*) is relative to a case where the two resonance frequencies f_m and f_e are not far from each other. Here we show two further representative examples of metalayers made of arrayed pairs of dogbone conductors, differently designed, by tailoring the conductor dimensions and the permittivity of the dielectric spacers, such that $f_e > f_m$and $f_m > f_e$, to demonstrate that our X-network can correctly predict the transmission and reflection behavior of a layer of paired dogbones in the general case.

Case 2: First, we show in Fig. 8 the case relative to a metalayer configuration in which the dielectric constant of the spacer is $\varepsilon_r = 1$. The dimensions of the unit cell and dogbone inclusions, made of copper, are as follows (in mm): $A = 7.5, B = 7.5, A1 = 1.0, B1 = 4, A2 = 7.4, B2 = 0.8, H = 0.2$.

Observing the results in Fig. 8, one should note that the transmission deep in the middle of the wide stop band is located around 9.2 GHz, which should approximately correspond to the electric resonance f_e. Around 11 GHz the reflection and transmission coefficients experience large and rapid variations, exhibiting almost total transmission and total reflection, in a very narrow frequency range, and as discussed in Section III this rapid variation should be close to the magnetic frequency f_m.

Through the steps described in Section II, the R, L and C parameters of the equivalent network are evaluated as

$$\begin{aligned} C_m &= 12.705 \text{ pF}, \quad L_m = 0.0165 \text{ nH}, \quad R_m = 497.119\ \Omega \\ C_e &= 0.0712 \text{ pF}, \quad L_e = 4.1807 \text{ nH}, \quad R_e = 0.252\ \Omega \end{aligned} \tag{21}$$

(note again that $C_m \gg C_e$ and $L_m \ll L_e$). The scattering parameters in Fig. 8 obtained from the TL model with the synthesized impedances of the X-network are in very good agreement with those obtained numerically. Now it is possible to derive a more precise value of the electric and magnetic frequencies as $f_e = 9.23$ GHz and $f_m = 10.98$ GHz.

The analysis described above is further confirmed in the case when both the conductors and the dielectric spacer are assumed lossless, for which T is plotted in the inset of Fig. 8, leading exactly to both total transmission $|T| = 1$ and total reflection $T = 0$, in a narrow frequency range near the magnetic resonance, as predicted by the theory in Section III.

Case 3: In the last example, shown in Fig. 9, the various geometrical parameters are (in mm): $A = 7.5, B = 7.5, A1 = 1.5, B1 = 4, A2 = 7.3, B2 = 0.8, H = 0.4$); the spacer between the pair of conductors has permittivity $\varepsilon_r = 4.5$ and $\tan\delta = 0.002$ (e.g., Rogers TMM4). The higher dielectric constant significantly decreases the resonance frequencies, and thus the location of the features shown in Fig. 9. Namely, the wide stop band around 7.5 GHz (associated with the electric resonance) and the rapid variation around 5.6 GHz (associated with the magnetic resonance).

Following the steps in Section II, the R, L and C parameters are evaluated as

$$\begin{aligned} C_m &= 20.344 \text{ pF}, \quad L_m = 0.0397 \text{ nH}, \quad R_m = 279.396\ \Omega \\ C_e &= 0.1509 \text{ pF}, \quad L_e = 3.0092 \text{ nH}, \quad R_e = 0.469\ \Omega \end{aligned} \tag{22}$$

Also in this case, $C_m \gg C_e$ and $L_m \ll L_e$, and the scattering parameters in Fig. 9 obtained from the TL model with the synthesized X-network are in good agreement with those obtained numerically. Once the L, C values are determined it is possible to retrieve the values of the magnetic and electric resonance frequencies: $f_m = 5.603$ GHz and $f_e = 7.47$ GHz. Therefore in this case $f_m < f_e$, similarly to the case in Fig. 2(a). In contrast to what happens in Fig. 2(a), besides the total reflection near f_e, here another reflection occurs slightly above f_m. This reflection as well as the peak of transmission that occurs near f_m. appear to be smoothed down by the high dielectric losses. However, in the absence of losses one should note that near the magnetic resonance both conditions $|T| = 1$ and $T = 0$ are exactly met, as shown in the inset of Fig. 9.

To conclude we can observe that in the first two cases (Figs. 2 and 8) the value of R_m is larger than $Z_0 \approx 377\ \Omega$. Therefore, considering the circuits in Figs. 3 and 7, neglecting losses (R_m) does not significantly affect the quality factor of the magnetic resonance Q_m and hence the performance of the metalayer. However, in the case shown in Fig. 9, R_m is smaller than $Z_0 \approx 377\ \Omega$ and therefore losses affect more significantly the metalayer performance, as shown in Fig. 9, where $|T|$ is smaller than unity.

In the following, on the basis of the analysis carried out in Section III, we summarize the matching and mismatching resonance conditions for the above sample dogbone pair metalayers.

A. Matching Conditions.

Case 1: In this case, relative to Fig. 2(a), one has $f_m < f_e$. The values in (4) determine the quality factors of the two resonances $Q_m = 82, Q_e = 0.32$, and the nondimensional parameters $a = 4.3 \times 10^{-3}$, $b = 3.6 \times 10^{-3}$. Now according to Table I, (11) and (15), the matching condition $|T| = 1$ occurs at $f_T = 6.333$ GHz, slightly (only 2 MHz) below the magnetic resonance at $f_m = 6.335$ GHz.

Case 2: On the contrary, in the case relative to Fig. 8 one has $f_e < f_m$. The values in (21) provide $Q_m = 330, Q_e = 0.64$, and $a = 1.6 \times 10^{-3}$, $b = 2.3 \times 10^{-3}$. According to Table I, (11) and (15), the matching condition $|T| \approx 1$ is verified at $f_T = 10.984$ GHz, that is slightly above f_m.

Case 3: In the case relative to Fig. 9 one has $f_m < f_e$. The values in (22) provide $Q_m = 269.8$, $Q_e = 0.375$, and $a = 0.19 \times 10^{-2}$, $b = 0.1 \times 10^{-2}$, which are even smaller than in the previous case, so that from (15), in the absence of losses, the matching condition $|T| = 1$ is encountered at $f_T = 5.601$ GHz, only 2 MHz below the magnetic resonance.

B. Total Reflection

Case 1: In this case, relative to Fig. 2, where $f_m < f_e$, the condition of total reflection (19) is not satisfied as $Q_m Q_e = 26.5 < 142$. Therefore, as apparent from Fig. 2, no total reflection occurs in this case.

Case 2: In the case relative to Fig. 8, where $f_e < f_m$, (19) is satisfied because $Q_m Q_e = 212 > 32.9$. Therefore, according to Table II and (20), the reflection condition $|R| \approx 1$ is satisfied at $f_{R_1} = 9.29$ GHz, slightly above f_e, and at $f_{R_2} = 10.90$ GHz, slightly below f_m. Hence, $f_{R_1} \approx f_e$ and $f_{R_2} \approx f_m$, with $f_e < f_{R_1} < f_{R_2} < f_m$, as expected.

Case 3: Lastly, in the case relative to Fig. 9, where $f_m < f_e$, (19) is satisfied as $Q_m Q_e = 101.15 > 12.02$. Therefore, two total reflections should occur in this case. According to Table II and (20), the reflection condition $|R| \approx 1$ is encountered at $f_{R_1} = 5.65$ GHz, slightly above f_m, and at $f_{R_2} = 7.404$ GHz, slightly below f_e. As shown in Fig. 9, while for lossy metals and dielectric spacer the reflection at f_{R_1} is attenuated, in the absence of losses at f_{R_1} we have exactly total reflection and $T = 0$ (cf. the inset in Fig. 9). In this case $f_m < f_{R_1} < f_{R_2} < f_e$.

V. Conclusion

In the context of a plane-wave transmission line model, we have synthesized a circuit network capable of reproducing the frequency response of a recently proposed metalayer made of a periodic arrangement of conductor pairs that possess a symmetric and an antisymmetric mode. The proposed circuit model provides for the first time a neat physical description of the transmission and reflection features of the metamaterial in terms of transmission lines and lumped elements. It also clarifies the relation between the peaks and stopbands in the transmission response and the main electric and magnetic resonances of the constituent paired conductors. The isolated transmission peak associated with the magnetic resonance in the middle of a wider stopband can be related to the Fano resonance observed in various studies.

The transmission line model can be generalized to oblique incidence angles, and even to predict surface and leaky modes in the metalayer studied in [26]. The transmission line model is also an effective tool to predict propagation through a number of layers. This network description offers the possibility to evaluate Bloch wavenumbers and characteristic impedances in metamaterials formed by stacked metalayers, and thus to match them to the free space impedance.

Though in this paper we analyze a layer made of pairs of dogbone shaped conductors, most of the results apply to other pair shapes as well, as long as there are two resonances in the metalayer: the symmetric and the antisymmetric one. Frequency selective surface properties may also benefit from the interplay of the two resonances explored in this paper.

It is finally observed that the proposed equivalent network can turn into an effective design tool provided that a connection between the circuit parameters and the geometrical parameters of the structure can be theoretically established, rather than resorting to curve fitting of simulated data. This can have a strong impact on the design of novel microwave devices, allowing to tailor the electric and magnetic resonance in a desired manner to realize, for example, wideband transparency and other intriguing properties. In [5] it has been suggested a method to predict the magnetic resonance, but the evaluation of the other parameters requires further investigations. However, whatever the method to retrieve the parameters will be found in the future, the proposed topology and conclusions will still remain fully valid.

Appendix

By using $L_e C_m = Q_m Q_e/(4\pi^2 f_e f_m)$, (18) is rearranged in the biquadratic form $f^4 - Bf^2 + f_m^2 f_e^2 = 0$, with $B = f_e^2 + f_m^2 - f_e f_m/(Q_m Q_e)$, which admits two real solutions for f in correspondence of positive real solutions for the quadratic equation $x^2 - Bx + f_m^2 f_e^2 = 0$ in $x \equiv f^2$. The two x-solutions are real for positive discriminants $B^2 - 4 f_m^2 f_e^2 \geq 0$. In addition, the two solutions $x_{1,2}$ satisfy $x_1 x_2 = f_m^2 f_e^2 > 0$, and therefore they are both either positive or negative. To have positive solutions $x_{1,2} \geq 0$, and in turn real f solutions, it must hold that $x_1 + x_2 = B \geq 0$. Combining these two condition one derives (19), and thus (20).

Acknowledgment

The authors thank Computer Simulation Technology (CST) for providing the simulation tool that was instrumental in this analysis.

References

[1] V. M. Shalaev, W. Cai, U. K. Chettiar, H. Yuan, A. K. Sarychev, V. P. Drachev, and A. V. Kildishev, "Negative index of refraction in optical metamaterials," *Opt. Lett.*, vol. 30, no. 24, pp. 3356–3358, Dec. 2005.

[2] J. Zhou, E. N. Economou, T. Koschny, and C. M. Soukoulis, "Unifying approach to left-handed material design," *Opt. Lett.*, vol. 31, no. 24, pp. 3620–3622, Dec. 2006.

[3] D. R. Smith, W. J. Padilla, D. C. Vier, S. C. Nemat-Nasser, and S. Schultz, "Composite medium with simultaneously negative permeability and permittivity," *Phys. Rev. Lett.*, vol. 84, pp. 4184–4187, 2000.

[4] J. Zhou, T. Koschny, L. Zhang, G. Tuttle, and C. M. Soukoulis, "Experimental demonstration of negative index of refraction," *Appl. Phys. Lett.*, vol. 88, p. 221103, 2006.

[5] G. Donzelli, A. Vallecchi, F. Capolino, and A. Schuchinsky, "Metamaterial made of paired planar conductors: Particle resonances, phenomena and properties," *Metamaterials*, vol. 3, no. 1, pp. 10–27, Mar. 2009.

[6] A. Vallecchi, F. Capolino, and A. Schuchinsky, "2-D isotropic effective negative refractive index metamaterial in planar technology," *IEEE Microwave Wireless Comp. Lett.*, vol. 19, no. 5, pp. 269–271, May 2009.

[7] A. Vallecchi and F. Capolino, "Tightly coupled tripole conductor pairs as constituents for a planar 2D-isotropic negative refractive index metamaterial," *Opt. Expr.*, vol. 12, no. 17, pp. 15216–15227, 2009.

[8] A. Vallecchi and F. Capolino, "Metamaterials based on pairs of tightly-coupled scatterers," in *Theory and Phenomena of Metamaterials*, F. Capolino, Ed. Boca Raton, FL: CRC Press, 2009.

[9] A. Vallecchi, F. Capolino, and M. Albani, "Metamaterial made of pairs of conductors in planar technology: A z-transmission line approach," presented at the Metamaterials 2008, Pamplona, Spain, Sep. 21–26, 2008.

[10] A. Vallecchi, M. Albani, and F. Capolino, "Planar metamaterial and its transverse equivalent network for application to low-profile antenna design," presented at the 3rd Eur. Conf. Antennas Propagat., EuCAP 2009, Berlin, Germany, Mar. 23–27, 2009.

[11] F. Capolino, A. Vallecchi, and M. Albani, "Transmission line model with X-circuit for a metamaterial layer made of pairs of dogbone-shaped planar conductors," presented at the Int. Symp. on Electromag. Theory EMTS 2010, Berlin, Germany, Aug. 16–19, 2010.

[12] E. A. Guillemin, *Synthesis of Passive Networks*. New York: Wiley, 1957.

[13] B. A. Munk, *Frequency Selective Surfaces: Theory and Design*. New York: Wiley, 2004.

[14] J. C. Vardaxoglou, *Frequency Selective Surfaces: Analysis and Design*. Taunton, England: Research Studies Press, 1997.
[15] R. M. Foster, "A reactance theorem," *Bell Syst. Tech. J.*, vol. 3, pp. 259–267, 1924.
[16] R. Rodríguez-Berral, F. Mesa, and F. Medina, "Circuit model for a periodic array of slits sandwiched between two dielectric slabs," *Appl. Phys. Lett.*, vol. 96, p. 161104, 2010.
[17] M. García-Vigueras, F. Mesa, F. Medina, R. Rodríguez-Berral, and J. L. Gómez-Tornero, "Equivalent circuits for conventional and extraordinary reflection in dipole arrays," presented at the Int. Microwave Symp., Baltimore, MD, Jun. 2011.
[18] S. Maci, M. Caiazzo, A. Cucini, and M. Casaletti, "A pole-zero matching method for EBG surfaces composed of a dipole FSS printed on a grounded dielectric slab," *IEEE Trans. Antennas Propag.*, vol. 53, no. 1, pp. 70–81, 2005.
[19] U. Fano, "Effects of configuration interaction on intensities and phase shifts," *Phys. Rev.*, vol. 124, p. 1866, 1961.
[20] V. A. Fedotov, M. Rose, S. L. Prosvirnin, N. Papasimakis, and N. I. Zheludev, "Sharp trapped-mode resonances in planar metamaterials with a broken structural symmetry," *Phys. Rev. Lett.*, vol. 99, no. 14, p. 147401, 2007.
[21] R. Singh, I. I. Al-Naib, M. Koch, and W. Zhang, "Sharp Fano resonances in THz metamaterials," *Opt. Expr.*, vol. 19, no. 7, pp. 6313–6319, 2011.
[22] S. Zhang, D. A. Genov, Y. Wang, M. Liu, and X. Zhang, "Plasmon-induced transparency in metamaterials," *Phys. Rev. Lett.*, vol. 101, p. 047401, 2008.
[23] J. A. Fan, K. Bao, C. Wu, J. Bao, R. Bardhan, N. J. Halas, V. N. Manoharan, G. Shvets, P. Nordlander, and F. Capasso, "Fano-like interference in self-assembled plasmonic quadrumer clusters," *Nano Lett.*, vol. 10, no. 11, pp. 4680–4685, 2010.
[24] D. F. Sievenpiper, J. H. Schaffner, H. J. Song, R. Y. Loo, and G. Tangonan, "Two-dimensional beam steering using an electrically tunable impedance surface," *IEEE Trans. Antennas Propag.*, vol. 51, no. 10, pp. 2713–2722, Oct. 2003.
[25] D. M. Pozar, *Microwave Engineering*, 3rd ed. Hoboken, NJ: Wiley, 2005.
[26] P. Baccarelli, F. Capolino, S. Paulotto, and A. Yakovlev, "In-plane modal analysis of a metamaterial layer formed by arrayed pairs of planar conductors," *Metamaterials*, vol. 5, pp. 26–35, 2011.

Filippo Capolino (S'94–M'97–SM'04) received the Laurea (*cum laude*) and the Ph.D. degrees in electrical engineering from the University of Florence, Italy, in 1993 and 1997, respectively.

He is currently an Associate Professor at the Department of Electrical Engineering and Computer. Science of the University of California, Irvine, USA. He has been an Assistant Professor at the Department of Information Engineering of the University of Siena, Italy. During 1997–1999, he was a Postdoctoral Fellow with the Department of Aerospace and Mechanical Engineering, Boston University, MA, USA. From 2000 to 2001 and in 2006, he was a Research Assistant Visiting Professor with the Department of Electrical and Comp. Engineering, University of Houston, TX. His research interests include antennas, metamaterials and their applications, sensors in both microwave and optical ranges, wireless systems, chip-integrated antennas. He has been the EU Coordinator of the EU Doctoral Programs on Metamaterials (2004–2009).

Dr. Capolino received the R. W. P. King Prize Paper Award from the IEEE Antennas and Propagation Society for the Best Paper of the Year 2000, by an author under 36. And he is a coauthor of the "Fast Breaking Papers, Oct. 2007" in E.E. and C.S., about metamaterials (paper that had the highest percentage increase in citations in Essential Science Indicators, ESI). He also received several young and senior scientist travel grants (IEEE and URSI) and two student and young scientist paper competition awards. In 2002–2008 he has served as an Associate Editor for the IEEE TRANSACTIONS ON ANTENNAS AND PROPAGATION. He is a founder and an Editor of the new journal *Metamaterials*, by Elsevier, since 2007. He is the Editor of the *Metamaterials Handbook*, CRC-Press, 2009.

Andrea Vallecchi received the Laurea (M.Sc.) degree *(summa cum laude*) in electronic engineering from the University of Florence, Florence, Italy, and the Ph.D. degree in information engineering, applied electromagnetics, and telecommunications from the University of Salerno, Salerno, Italy.

He then worked at the Laboratory of Antennas and Microwaves of the University of Florence, as a research associate, and subsequently, since 2007, has been a postdoctoral research fellow at the University of Siena. In 2009 he spent some months working as an assistant specialist at the University of California, Irvine, USA. In 2009 and 2010 he was a Visiting Researcher at Queen's University of Belfast, Belfast, U.K. He is currently with the Department of Information Engineering, University of Siena. His present research interests are in the theoretical characterization and design of metamaterials for applications at microwaves and optical frequencies.

Matteo Albani (M'98–SM'10) received the Laurea degree (*cum laude*) in electronic engineering (1994) and the Ph.D. degree in telecommunications engineering (1999) from the University of Florence, Italy.

From 2001 to 2005 he was with the University of Messina, Italy, as an Assistant Professor. Since 2005, he has been an Aggregate Professor with the Information engineering Department, University of Siena, Italy, where he is also Director of the Applied Electromagnetics Lab. His research interests are in the areas of high-frequency methods for electromagnetic scattering and propagation, electromagnetic modeling for metamaterials, antenna design.

Dr. Albani was awarded the "Giorgio Barzilai" prize for the Best Young Scientist paper at the Italian National Conference on Electromagnetics in 2002 (XIV RiNEm).